◆ Human Brain Mapping 36:3749–3760 (2015) ◆

Effect of In-Painting on Cortical Thickness Measurements in Multiple Sclerosis: A Large Cohort Study

Koushik A. Govindarajan,[1] Sushmita Datta,[1] Khader M. Hasan,[1] Sangbum Choi,[2] Mohammad H Rahbar,[2] Stacey S. Cofield,[3] Gary R. Cutter,[3] Fred D. Lublin,[4] Jerry S. Wolinsky,[5] and Ponnada A. Narayana,[1]* MRI Analysis Center at Houston, The CombiRx Investigators Group

[1]Department of Diagnostic and Interventional Imaging, University of Texas Medical School at Houston, Houston, Texas
[2]Division of Clinical and Translational Sciences, Internal Medicine, University of Texas Medical School at Houston, Houston, Texas
[3]Department of Biostatistics, University of Alabama at Birmingham, Birmingham, Alabama
[4]The Corinne Goldsmith Dickinson Center for Multiple Sclerosis, Mount Sinai School of Medicine, New York, New York
[5]Department of Neurology, University of Texas Medical School at Houston, Houston, Texas

MRI Analysis Center: JS Wolinsky, PA Narayana, F Nelson, I Vainrub, S Datta, R He, B Gates, K Ton.

CombiRx Investigators Group: M. Agius, Sacramento, CA; K. Bashir, Birmingham, AL; R. Baumhefner, Los Angeles, CA; G. Birnbaum, Golden Valley, MN; G. Blevins, Edmonton, AB, Canada; R. Bomprezzi, Phoenix, AZ; A. Boster, Columbus, OH; T. Brown, Kirkland, WA; J. Burkholder, Canton, OH; A. Camac, Lexington, MA; D. Campagnolo, Phoenix, AZ; J. Carter, Scottsdale, AZ; B. Cohen, Chicago, IL; J. Cooper, Berkeley, CA; J. Corboy, Aurora, CO; A. Cross, Saint Louis, MO; L. Dewitt, Salt Lake City, UT; J. Dunn, Kirkland, WA; K. Edwards, Latham, NY; E. Eggenberger, East Lansing, MI; J. English, Atlanta, GA; W. Felton, Richmond, VA; P. Fodor, Colorado Springs, CO; C. Ford, Albuquerque, NM; M. Freedman, Ottawa, Ontario, Canada; S. Galetta, Philadelphia, PA; G. Garmany, Boulder, CO; A. Goodman, Rochester, NY; M. Gottesman, Mineola, NY; C. Gottschalk, New Haven, CT; M. Gruental, Albany, NY; M. Gudesblatt, Patchogue, NY; R. Hamill, Burlington, VT; J. Herbert, New York, NY; R. Holub, Albany, NY; W. Honeycutt, Maitland, FL; B. Hughes, Des Moines, IA; G. Hutton, Houston, TX; D. Jacobs, Philadelphia, PA; K. Johnson, Baltimore, MD; L. Kasper, Lebanon, NH; J. Kattah, Peoria, IL; M. Kaufman, Charlotte, NC; M. Keegan, Rochester, NY; O. Khan, Detroit, MI; B. Khatri, Milwaukee, WI; M. Kita, Seattle, WA; B. Koffman, Toledo, OH; E. Lallana, Lebanon, NH; N. Lava, Albany, NY; J. Lindsey, Houston, TX; P. Loge, Billings, MT; S. Lynch, Kansas City, KS; F. McGee, Richmond, VA; L. Mejico, Syracuse, NY; L. Metz, Calgary, AB, Canada; P. O'Connor, Toronto, ON, Canada; K. Pandey, Albany, NY; H. Panitch, Burlington, VT; J. Preiningerova, New Haven, CT; K. Rammohan, Columbus, OH; C. Riley, New Haven, CT; P. Riskind, Worcester, MA; L. Rolak, Marshfield, WI; W. Royal, Baltimore, MD; S. Scarberry, Fargo, ND; A. Schulman, Richmond, VA; T. Scott, Pittsburgh, PA; C. Sheppard, Uniontown, OH; W. Sheremata, Miami, FL; L. Stone, Cleveland, OH; W. Stuart, Atlanta, GA; S. Subramaniam, Nashville, TN; V. Thadani, Lebanon, NH; F. Thomas, Saint Louis, MO; B. Thrower, Atlanta, GA; M. Tullman, New York, NY; A. Turel, Danville, PA; T. Vollmer, Phoenix, AZ; S. Waldman, La Habra, CA; B. Weinstock-Guttman, Buffalo, NY; J. Wendt, Tucson, AZ; R. Williams, Billings, MT; D. Wynn, Northbrook, IL; M. Yeung, Calgary, AB Canada.

Koushik A. Govindarajan and Sushmita Datta contributed equally to this work.

Contract grant sponsor: NINDS/NIH; Contract grant number: R01NS078244; Contract grant sponsor: NINDS/NIH (CombiRx trial); Contract grant number: U01 NS045719; Contract grant sponsor: NIBIB/NIH (Image segmentation); Contract grant number: 2 R01 EB02095

*Correspondence to: Ponnada A. Narayana, Department of Diagnostic and Interventional Imaging, University of Texas Medical School at Houston, 6431 Fannin Street, Houston, Texas.
E-mail: Ponnada.a.narayana@uth.tmc.edu

Received for publication 27 January 2015; Revised 27 April 2015; Accepted 1 June 2015.

DOI: 10.1002/hbm.22875

Published online 19 June 2015 in Wiley Online Library (wileyonlinelibrary.com).

Abstract: A comprehensive analysis of the effect of lesion in-painting on the estimation of cortical thickness using magnetic resonance imaging was performed on a large cohort of 918 relapsing-remitting multiple sclerosis patients who participated in a phase III multicenter clinical trial. An automatic lesion in-painting algorithm was developed and implemented. Cortical thickness was measured using the FreeSurfer pipeline with and without in-painting. The effect of in-painting was evaluated using FreeSurfer's paired analysis pipeline. Multivariate regression analysis was also performed with field strength and lesion load as additional factors. Overall, the estimated cortical thickness was different with in-painting than without. The effect of in-painting was observed to be region dependent, more significant in the left hemisphere compared to the right, was more prominent at 1.5 T relative to 3 T, and was greater at higher lesion volumes. Our results show that even for data acquired at 1.5 T in patients with high lesion load, the mean cortical thickness difference with and without in-painting is ~2%. Based on these results, it appears that in-painting has only a small effect on the estimated regional and global cortical thickness. *Hum Brain Mapp 36:3749–3760, 2015.*

Key words: cortical thickness; FreeSurfer; lesion in-painting; multiple sclerosis lesions; multiple sclerosis

INTRODUCTION

Multiple sclerosis (MS) is the most common neurological disease in young adults. It is characterized by the presence of white matter (WM) and gray matter (GM) lesions. On conventional magnetic resonance imaging (MRI), WM lesions which appear hyperintense on T2-weighted images (T2 lesions) are most common and GM lesions are less frequently observed in MS. The hyperintense WM lesions consist of two components: those which appear hypointense (generally referred to as T1 lesions) and those which appear iso-intense on the T1-weighted images (referred to as T2 lesions). Generally, the volume of the T1 lesions is only a small fraction of the T2 lesions. Another hallmark of MS pathology is cortical thinning that is thought to be an early feature of the disease [Calabrese et al., 2010; Charil et al,. 2007; Narayana et al., 2013; Sailer et al., 2003]. It is therefore not surprising that cortical thinning in MS has recently attracted considerable attention.

MRI is most commonly used for determining regional and global cortical thicknesses. With the free availability of powerful software packages such as FreeSurfer (http://surfer.nmr.mgh.harvard.edu/fswiki) [Dale et al., 1999; Fischl et al., 1999] cortical thickness can be routinely measured on three-dimensional (3D) T1-weighted MRI brain scans. The pipeline for measuring the cortical thickness includes nonlinear registration of individual image volumes to an atlas.

The presence of lesions affects the quality of registration that may bias the measured cortical thickness [Battaglini et al., 2012; Ceccarelli et al., 2012; Chard et al., 2010; Sdika and Pelletier, 2009]. The majority of tissue segmentation algorithms classify perilesional areas as GM [Sajja et al., 2006; Shiee et al., 2014]. This can also affect the measured cortical thickness, particularly if the lesions are close to the cortex [Magon et al., 2014]. Lesion in-painting is thought to mitigate this problem to some extent [Battaglini et al., 2012; Ceccarelli et al., 2012; Chard et al., 2010; Magon et al., 2014; Sdika and Pelletier 2009]. Image in-painting is commonly used for removing certain undesirable features such as scratches and unwanted scenes and replace them without disturbing the overall visual appearance [Ballester et al., 2001]. A similar strategy can be applied to remove lesions and replace them with surrounding tissues. In-painting can be performed by replacing the lesion voxels with (1) an average of neighboring voxels, (2) adjacent normal appearing WM voxel intensities using *a priori* information, and (3) intensity of the mean WM over the entire brain. Sdika and Pelletier [2009] demonstrated improvement in nonrigid registration and morphometric measurements following lesion in-painting in five MS patients using the second method. Based on simulations, Chard et al. [2010] showed improvement in GM and WM volumes following lesion in-painting. Ceccarelli et al. [2012] reported, based on 26 relapsing remitting MS (RRMS) patients, improvement in the image segmentation and detection of regional atrophy. Datta et al. [2014], based on a large RRMS cohort, demonstrated that the effect of lesion in-painting was most evident on regional atrophy in patients with high lesion load.

The literature on the effect of in-painting on cortical thickness is sparse. Recently, Magon et al. [2014], based on cross-sectional and longitudinal studies on 50 MS patients, reported that the presence of WM lesions introduces a bias in the cortical thickness. Shiee et al. [2014], proposed an automated method for lesion-filling to overcome the inaccuracy in cortical thickness estimation due to WM lesions. Both the above studies were carried out on data acquired from a single 1.5 T scanner and did not account for the variability that arises from the scanner field strength, lesion load, and other confounders [Wonderlick et al., 2009; Govindarajan et al., 2014]. Previous studies by Han et al. [2006] and Dickerson et al. [2009] showed the variability in

the measurement of cortical thickness between data acquired at 1.5 T and 3 T.

Lesion in-painting involves an additional processing step. Based on the studies by Datta et al. [2014] lesion in-painting on regional atrophy is relatively modest, particularly when the lesion load is low. However, the effect of lesion load on cortical thickness is not investigated so far. The importance of in-painting on MRI-based cortical thickness measurements needs to be evaluated on a large cohort because of the patient heterogeneity. Acquisition of data on large cohorts involves subject recruitment by multiple centers with different scanners operating at different field strengths, vendors, and pulse sequences. All these variables could have an effect on the influence of lesion in-painting. A large sample size allows us to include theses confounders on the evaluation of lesion in-painting on cortical thickness. In this study, we analyzed the effect of lesion in-painting in a large cohort of 918 RRMS patients who participated in a multicenter clinical trial. We also investigated the effect of scanner field strength, and lesion load on the effect of in-painting on cortical thickness. We believe that this is the first comprehensive study that investigated the effect of lesion in-painting on cortical thickness in a large patient cohort.

METHODS

Subjects

This study included 918 RRMS patients who participated in the CombiRx clinical trial (NCT00211887). CombiRx is a multicenter, double-blinded randomized clinical trial sponsored by the National Institutes of Neurological Disorders and Stroke. The primary focus of this clinical trial was to evaluate the efficacy of interferon beta-1a and glatiramer acetate as individual agents versus combined dosage [Lindsey et al., 2012].

MRI Protocol

The CombiRx MRI protocol included the acquisition of two-dimensional (2D) fluid attenuated inversion recovery (FLAIR), dual echo fast spin echo (FSE), precontrast and postcontrast T1 images (all with voxel dimensions of 0.94 mm $\times$ 0.94 mm $\times$ 3 mm). In addition, 3D T1 spoiled gradient recalled echo (SPGR)/magnetization prepared rapid acquisition of gradient echo (MPRAGE) images were also acquired with a voxel size of 0.94 mm $\times$ 0.94 mm $\times$ 1.5 mm.

MRI Quality Assurance

Inconsistency in image quality is not uncommon in multicenter studies. It is extremely tedious to manually evaluate each image set for quality. Therefore, a pipeline was implemented for automatic evaluation of the image quality [Narayana et al., 2013]. Images with poor signal-to-noise ratio and/or artifacts such as ghosting are automatically identified. This pipeline also reads the DICOM header for detecting the MRI protocol violations. These flagged images were then manually inspected to evaluate their suitability for inclusion in the analysis.

Lesion Segmentation

Image processing and segmentation were performed using an in-house developed pipeline, magnetic resonance image automatic processing [Datta et al., 2006; Sajja et al., 2006]. Briefly, the 2D FLAIR, T1 precontrast and postcontrast contrast images were coaligned with the 2D dual echo FSE images using rigid body registration. These images were skull-stripped, bias corrected, and intensity standardized. A unified approach that combines nonparametric and parametric techniques was used to classify T2 hyperintense lesions, cerebrospinal fluid (CSF), and normal tissues including WM and GM [Sajja et al., 2006]. The WM lesions were segmented as described by Datta et al. [2007]. The lesion segmentation results were validated by experienced neurologist (JSW) and imaging scientists (PAN, SD) as a part of the QA procedure.

Lesion In-Painting

The 3D T1 images were skull-stripped using BET [Smith, 2002] and bias corrected. Affine transformation was applied to the T1 precontrast images (previously aligned with FSE) to align with the 3D T1 images. The transformation matrix obtained from the affine transformation was applied to the 2D segmented images to transform them into the 3D T1 space. The aligned 3D segmented images were used to generate the WM and lesion masks. The WM mask was applied to the 3D T1 image volume to obtain the WM intensity profile. A set of WM intensities, say X, at full width at half maximum was obtained which were used to replace the voxel intensities corresponding to the lesion areas on the 3D T1 image. The intensity of each voxel in the 3D images was replaced by intensity selected randomly from the set X. Gaussian filter was applied to lesion area following the replacement of voxel intensity to minimize the effect of the noise due to random assignment of intensity values. This results in lesion in-painted 3D T1 image showing normal tissue intensities [Datta et al., 2014].

Cortical Thickness Estimation

Cortical thickness was determined using the FreeSurfer pipeline (v5.1.0; http://surfer.nmr.mgh.harvard.edu/fswiki) [Dale et al., 1999; Fischl et al., 1999] on a Linux platform. Briefly, the automated FreeSurfer pipeline involves resampling of the 3D T1-weighted images to a 1 mm isotropic voxel, followed by intensity normalization. Further, the MRI

TABLE I. Demographic information on 918 RRMS patients

		1.5 T	3 T
N (low/high lesion volume)	918 (459/459)	663 (334/329)	255 (125/130)
Gender (M, %)	246 (27%)	172 (26%)	74 (29%)
Age (Mean ± SD; Range)	37.5 ± 9.6; 18–61	37.8 ± 9.4; 18–61	36.9 ± 9.9; 18–60
Lesion volume (Mean ± SD; Range)	10.5 ± 11.5; 0.06–76.2	10.4 ± 11.5; 0.06–76.2	10.8 ± 11.6; 0.3–58.1

data are registered to the Montreal Neurological Institute space [Collins et al., 1994] using a 12-parameter affine transformation. The images are skull stripped using a hybrid algorithm that combines watershed with the deformable template model [Ségonne et al., 2004]. An initial estimation of the surfaces is constructed, based on a validated algorithm [Dale et al., 1999; Fischl et al., 1999, 2001]. An automatic algorithm is then employed to correct topological defects before generating the final white and pial surfaces. All the FreeSurfer output images were visually inspected for artifacts and quality of segmentation. Cortical thickness is defined as "the average of the distance between the surface (pial) and the GM–WM boundary and the distance between the GM–WM boundary and the surface (pial)" [Fischl and Dale, 2000]. The images are then transformed into a spherical space on which the parcellation of the cortical regions is performed. In this study, we used the labels based on the Desikan–Killiany atlas [Desikan et al., 2006] for lobar cortical thickness measurements. Cortical thickness and other measurements are then estimated in the subject space. Cortical thicknesses were determined separately with and without in-painting. FreeSurfer divides each hemisphere into 34 cortical regions. To reduce the complexity of the results, we reported results on six regional structures: frontal, parietal, occipital, and temporal lobes, and insular and cingulate cortices.

Classification by Magnetic Field Strength

The subjects were divided into two groups based on the field strength at which the images were acquired. This classification is necessary because earlier studies [Dickerson et al., 2009; Govindarajan et al., 2014; Han et al., 2006] showed that the estimated cortical thickness depends on the field strength.

Classification by Lesion Extent

As the effect of lesion in-painting may depend on the lesion load, we divided the sample of 918 patients into two subgroups (low and high) based on the median value of the WM lesion volumes. The sample within both the subgroups was further subdivided based on the two field strengths.

Statistical Analysis

Statistical difference maps (with and without in-painting) were generated using the FreeSurfer group analysis module. The surface maps were smoothed using a kernel with a FWHM of 10 mm based on the developers' recommendation. Monte Carlo simulation with 5,000 iterations was used to draw inferences at $P = 0.01$ with a false discovery rate of $P < 0.05$. These analyses were performed for the whole group (918 patients) and at each field strength separately.

Multivariate regression analysis [Hand and Taylor, 1987; Krzanowski, 1988] was performed to evaluate the relationship between cortical thickness and several factors. Specifically, we considered differences between in-painted and nonpainted regional cortical thickness for left and right hemispheres as a vector of dependent variable and treated field strength, and T2 lesion volume as independent variables. To compare multivariate population means of cortical thickness among 34 regions parcellated by FreeSurfer, with and without in-painting, we applied multivariate analysis of variance, which is used when there are two or more dependent variables and provides individual *P*-values for each dependent variable to test for statistical significance. Statistical significance was evaluated using Pillai's trace test [Olson, 1974]. To check region-specific effect, we also considered single linear regression and analysis of variance (ANOVA) for each region. We used "fieldtype" to denote the type of field strength, where fieldtype = 0 and 1 indicate 1.5 T and 3 T field strengths, respectively. For pulse sequence, we considered MPRAGE and SPGR as one category [Govindarajan et al., 2014; Narayana et al., 2013]. To assess the effect of lesion volumes on cortical thickness, we divided the subjects into two groups based on the median of lesion volumes. The vectors of coefficients from multivariate regression model, controlling for potential confounding or effect modifications, were estimated. The adjusted means and mean differences between regional cortical thicknesses along with *P*-values for comparison were calculated. All the above analyses were performed using SAS 9.3 (http://www.sas.com; Cary, NC).

The retrospective analysis of the data presented in this manuscript was approved by our Institution Review Board.

RESULTS

Subjects

Of the 918 subjects, 672 were females and 246 males. They were in the age range of 18–61 years (Mean: 37.5; Median: 37; SD: 9.57). Six hundred and sixty three subjects

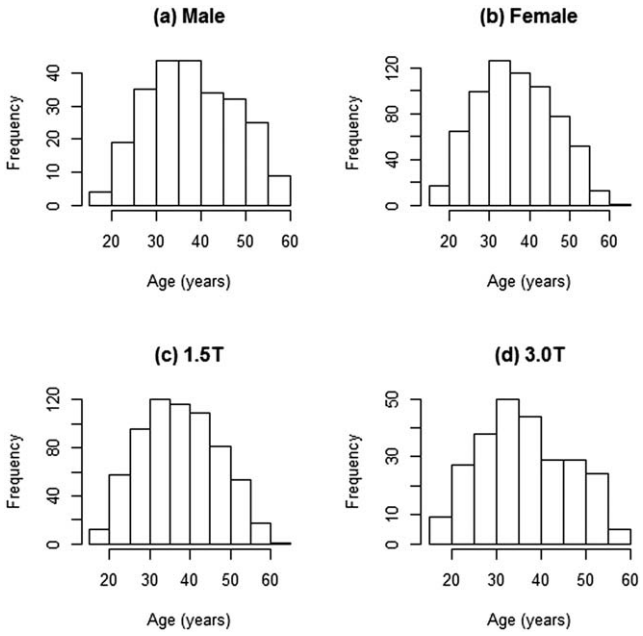

Figure 1.
Age distribution of RRMS patients by gender and field strength.

were scanned at 1.5 T and 255 at 3 T. Table I summarizes the demographic data, scanner field strength, and the WM lesion volumes (or lesion load). Figure 1 shows the histogram of age distribution of the cohort by gender and field strength.

Lesion Segmentation and In-Painting

Figure 2 shows, as an example, the original T1 image, in-painted image, and color-coded segmented image. The color-coded image shows WM (white), GM (gray), CSF (blue), T2 lesions (pink), and T1 lesions (dark red). The lesions are completely absent on the in-painted images. The histogram distributions for the low and high lesion volume subgroups are also shown in Figure 3. The estimated total WM lesion load in our sample was in the range of 0.06–76.23 ml with a median value of 6.42 ml (Fig. 3).

Cortical lesions (juxtacortcal and intracortical lesions) are expected to have a significant effect on the estimated cortical thickness. However, it is very difficult to visualize intracortical lesions on FLAIR and FSE images [Geurts et al., 2005; Nelson et al., 2011]. We paid particular attention if our software can segment out the juxtacortical lesions. Figure 4 shows examples of juxtacortical lesion segmentation on two different patients. It can be observed on these figures that our software identified the juxtacortical lesions and that these lesions are not always clearly visualized on T1-weighted images even though the latter were acquired at higher spatial resolution compared to FLAIR and FSE images.

Effect of In-Painting on Cortical Thickness

Figure 5 shows the difference map between in-painted and nonpainted whole groups on an inflated brain surface at a *P*-value of 0.01. The multiple lobes are shown in different colors for differentiating their topological boundaries. As can be seen from this figure, the effect of in-painting appears to be different between the right and left hemispheres. For example, almost the entire insular cortex and significant parts of the frontal, parietal and temporal lobes are affected in the left hemisphere. However, the structures affected by in-painting in the right hemisphere include smaller regions in the temporal, parietal, frontal, and insular regions. The results of the statistical analysis

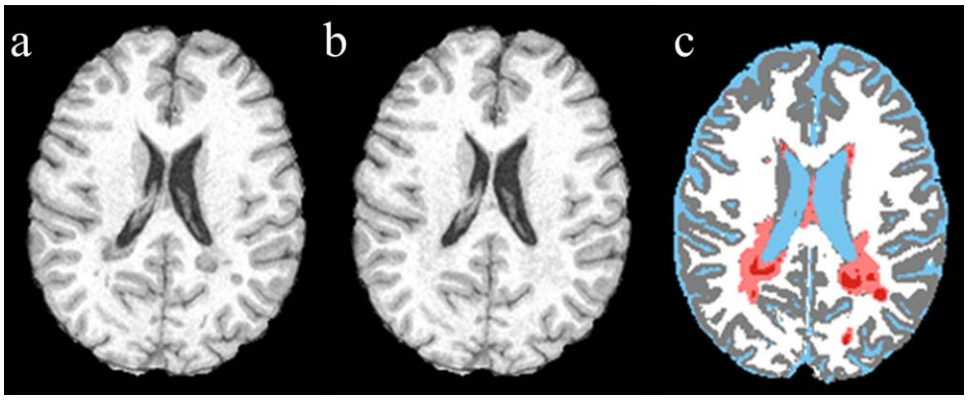

Figure 2.
An axial slice of original (left), in-painted (middle), and segmented (right) image. In the color-coded image WM, GM, CSF, T2-lesions, and T1-hypointense lesions are indicated by white, gray, blue, pink, and red, respectively. [Color figure can be viewed in the online issue, which is available at wileyonlinelibrary.com.]

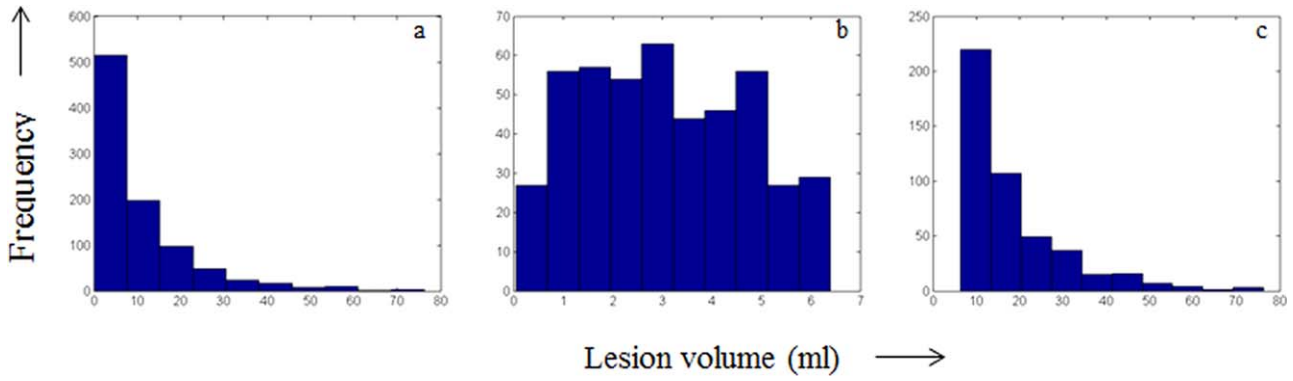

Figure 3.
Lesion volume distribution in the RRMS patients (**a**) whole group, (**b**) low lesion volume, and (**c**) high lesion volume. [Color figure can be viewed in the online issue, which is available at wileyonlinelibrary.com.]

on the entire group of in-painted versus nonpainted subjects are summarized in Table II. All lobes excluding the parietal lobe in the left hemisphere showed significant differences. In contrast, temporal, occipital, cingulate, and insular regions in the right hemisphere were significantly affected by in-painting. Overall, the extent of differences between the in-painted and nonpainted groups was different between the two hemispheres—the left hemisphere showing greater differences than the right hemisphere in many lobar regions. *P*-values for Pillai's trace test in Table III indicate statistically significant differences in cortical thickness between in-painted and nonpainted groups. Difference by the WM lesion volume seems evident in left hemisphere but not on the right. To understand if these differences between the two hemispheres are related to the possible asymmetric distribution of lesions in the two

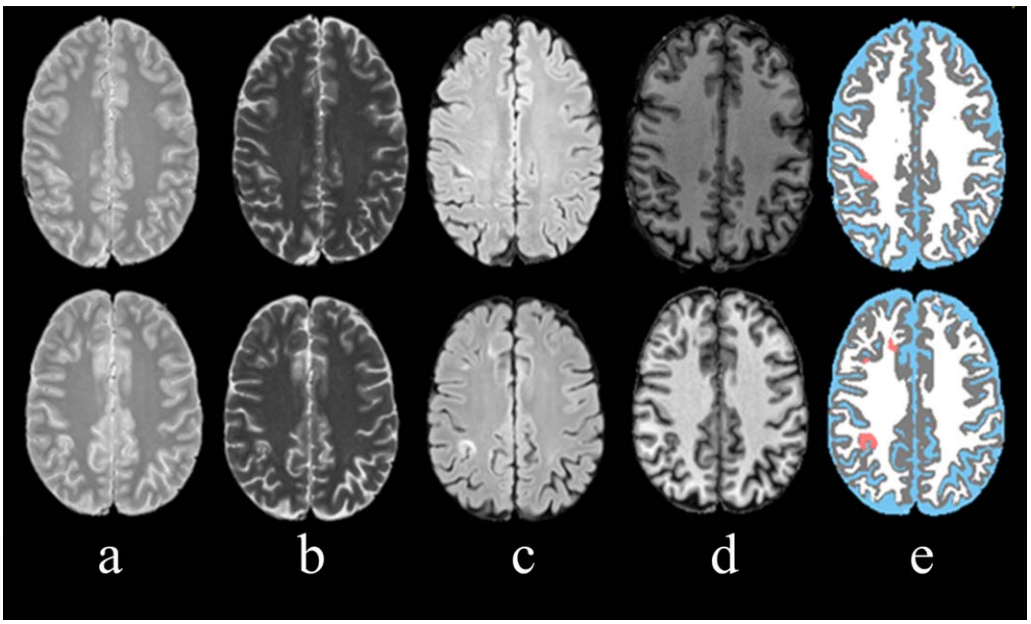

Figure 4.
Images showing segmentation of juxtacortical lesions on two patients (top and bottom rows). (**a**) Short echo FSE, (**b**) long echo FSE, (**c**) FLAIR, (**d**) 3DT1, and (**e**) segmented images. In the color-coded segmented image WM, GM, CSF, and lesions are indicated by white, gray, blue, and red, respectively. [Color figure can be viewed in the online issue, which is available at wileyonlinelibrary.com.]

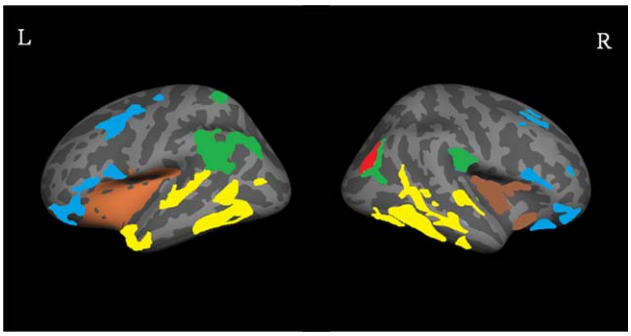

Figure 5.
Lateral views of inflated left (L) and right (R) hemispheres depicting group difference maps highlighting significantly thinner regions in nonpainted images compared to lesion in-painted images. The different lobes are denoted in different colors: frontal (blue), temporal (yellow), parietal (green), occipital (red), and insula (brown). [Color figure can be viewed in the online issue, which is available at wileyonlinelibrary.com.]

hemispheres, we calculated the lesion probability distribution. Figure 6a shows the lesion distribution map in the whole group. Figure 6b,c show the lesion distribution map for the data from 1.5 T and 3 T. No significant asymmetry in the lesion distribution between the two hemispheres in the two subgroups of the patients is apparent.

Table IV summarizes the results of multivariate regression analysis performed on six different lobes/structures. In the left hemisphere, differences between the in-painted and nonpainted groups were significant for frontal, parietal, temporal, cingulate, and insula regions at a 0.01 significance level, whereas in the right hemisphere, differences were significant for frontal, temporal, occipital, cingulate, and insula. The mean difference values indicate that excluding the occipital lobe, all the other regions had a higher cortical thickness without in-painting than with in-painting. This directionality was reversed for the occipital lobe in both hemispheres. Difference by field strength was found only in the cingulate and insula in the left hemisphere and occipital lobe in the right hemisphere. Differences due to lesion volume were significant in parietal and occipital lobes in both hemispheres and left temporal and right frontal lobes.

Subgroup Analysis of the Effect of Field Strength and Lesion Load

The effect of in-painting is different at the two field strengths. Figure 7 shows that at 1.5 T, significant differences were observed in the frontal, parietal, temporal, occipital, and insula regions while the results at 3 T indicate much smaller differences in parts of the frontal, temporal, and insula regions. Table V summarizes the results of multivariate regression analysis on the effect of in-painting on cortical thickness stratified by field strength. In the left hemisphere, frontal, temporal, cingulate, and insula and in the right hemisphere, temporal, occipital, cingulate, and insula showed significant differences. The significant differences due to field strength were observed in the temporal and occipital regions in both the hemispheres and the left cingulate.

Figure 7 also shows the significant differences between in-painted and nonpainted brains classified by lesion volumes. The results indicate that at high lesion volumes, there is a greater difference between in-painted and nonpainted brains, particularly at 1.5 T. The results from the multivariate regression analysis showing the cortical thickness differences stratified by lesion volumes are summarized in Table VI. In the left hemisphere, frontal, temporal, cingulate, and insula were significant and in the right hemisphere, only the temporal lobe was significant. The significant differences due to lesion volume were observed in the frontal, parietal, and temporal lobes in both hemispheres.

DISCUSSION

In this study, we evaluated the effect of in-painting on the cortical thickness in a large cohort of 918 RRMS patients. Our analysis also included the effects of field strength and lesion load on the cortical thickness. To our knowledge, this is the largest sample size ever used for such an analysis. The major findings of this study are that the effect of in-painting (1) results in differences in the

TABLE II. Average cortical thickness with and without in-painting on 918 RRMS patients

	Thickness (mm), Left hemisphere				Thickness (mm), Right hemisphere			
Lobe	In-painted	Nonpainted	Difference	*P*-value	In-painted	Nonpainted	Difference	*P*-value
Frontal	2.547 ± 0.229	2.563 ± 0.215	−0.016	0.0007	2.559 ± 0.22	2.561 ± 0.218	−0.002	0.6386
Parietal	2.315 ± 0.213	2.321 ± 0.202	−0.006	0.3112	2.326 ± 0.211	2.319 ± 0.198	0.007	0.2723
Temporal	2.687 ± 0.28	2.723 ± 0.253	−0.036	<0.0001	2.742 ± 0.281	2.767 ± 0.265	−0.025	0.0012
Occipital	1.959 ± 0.22	1.938 ± 0.198	0.021	0.0050	1.996 ± 0.215	1.978 ± 0.193	0.018	0.0155
Cingulate	2.624 ± 0.27	2.661 ± 0.251	−0.037	<0.0001	2.624 ± 0.27	2.646 ± 0.245	−0.022	0.0071
Insula	2.955 ± 0.266	3.017 ± 0.296	−0.062	0.0001	2.968 ± 0.271	3.003 ± 0.284	−0.035	0.0255

The difference in cortical thickness (in-painted–nonpainted) is also shown.

TABLE III. Results from multivariate ANOVA (*P*-values for Pillai's trace test)

	Left hemisphere	Right hemisphere
Difference in cortical thickness (in-painted vs. nonpainted)	<0.0001	0.00014
Field strength (3 T vs. 1.5 T)	0.2148	0.0424
T2 lesion volume	0.0295	0.4488

estimation of cortical thickness, (2) is different for the left and right hemispheres, (3) depends on the lesion load, and (4) is more prominent at 1.5 T compared to 3 T.

As discussed below, there are at least three reasons why in-painting may have an effect on the measured cortical thickness:

1. *Nonlinear registration*: Cortical thickness determination involves registration of MS brain images to a normal atlas. As the normal brain does not have lesions while the MS brain does, nonlinear registration could introduce errors that in turn might affect the calculated cortical thickness. As shown by Sdika and Pelletier [2009] lesion in-painting reduces the registration errors.
2. *Partial volume averaging*: Given the thinness of the cortical ribbon and its convoluted geometry, partial volume averaging between WM and GM exists even at 1-mm isotropic voxel resolution. Contrast-to-noise ratio (CNR) has a significant effect on the measured cortical thickness. CNR between the WM and cortical GM can be formally defined as the signal intensity difference between these two tissues divided by noise standard deviation [Bock et al., 2013; Lu et al., 2005]. Mathematically, CNR can be expressed as

$$\mathrm{CNR} = \left[S_{\mathrm{wm}} - S_{\mathrm{gm}}\right]/\mathrm{Noise} = k * B_0 * \left(1/\sqrt{(\mathrm{T1_{wm}})} - 1/\sqrt{(\mathrm{T1_{gm}})}\right) \quad (1)$$

where k is a constant that depends on the voxel volume and the (number of averages)$^{1/2}$ and B_0, the magnetic field strength. In the above equation, S_{wm} and S_{gm} denote signals from WM and GM, respectively, and the corresponding longitudinal relaxation times are $\mathrm{T1_{wm}}$ and $\mathrm{T1_{gm}}$. It can be seen from the above equation that the CNR depends on tissue T1. As the T1 value of GM is larger than that of WM, partial volume averaging between WM and GM

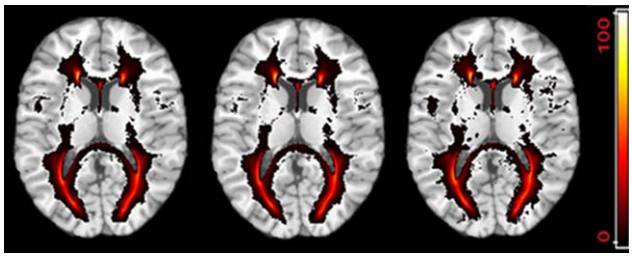

Figure 6.
Lesion distribution maps in RRMS patients in the whole group and at each of the two field strengths. The temperature bar indicates the lesion probability. [Color figure can be viewed in the online issue, which is available at wileyonlinelibrary.com.]

TABLE IV. Multivariate regression on cortical thickness with and without in-painting on 918 RRMS patients

Lobe	Parameter	Mean difference in cortical thickness	*P*-value, Left hemisphere (in-painted vs. nonpainted)	Mean difference in cortical thickness	*P*-value, Right hemisphere (in-painted vs. non-painted)
Frontal	Intercept	−0.024	<0.0001	−0.012	0.0009
	Field strength	0.010	0.0672	0.003	0.5453
	Lesion load	0.011	0.0233	0.019	0.0001
Parietal	Intercept	−0.018	0.0001	−0.006	0.214
	Field strength	0.014	0.0183	−0.002	0.7450
	Lesion load	0.016	0.0049	0.026	<0.0001
Temporal	Intercept	−0.052	<0.0001	−0.035	<0.0001
	Field strength	0.016	0.0425	0.009	0.2331
	Lesion load	0.026	0.0001	0.016	0.0304
Occipital	Intercept	0.007	0.2565	0.016	0.0077
	Field strength	0.001	0.8642	−0.025	0.0035
	Lesion load	0.028	0.0005	0.019	0.0097
Cingulate	Intercept	−0.046	<0.0001	−0.026	0.0002
	Field strength	0.028	0.0059	0.010	0.3049
	Lesion load	0.001	0.9222	0.002	0.8523
Insula	Intercept	−0.072	<0.0001	−0.054	0.0006
	Field strength	0.056	0.0084	0.057	0.0120
	Lesion load	−0.013	0.4893	0.008	0.6773

Intercept represents the significant difference in the cortical thickness measures with and without in-painting.

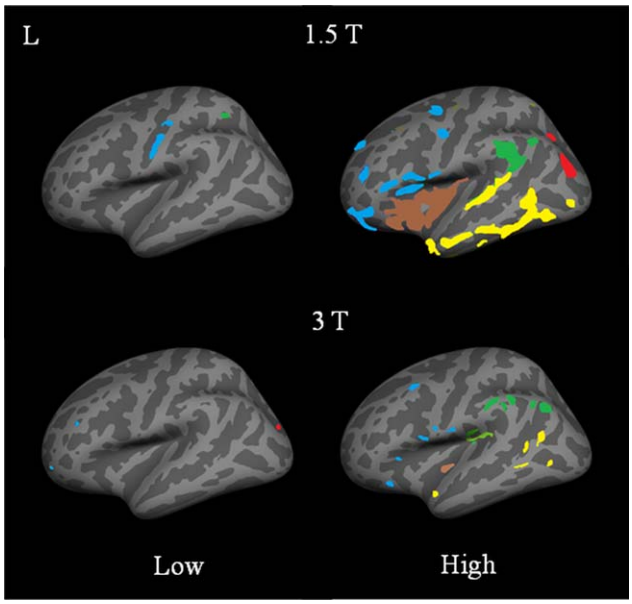

Figure 7.
Lateral views of inflated left (L) hemisphere grouped by lesion load for 1.5 T and 3 T data. Images depict group difference maps highlighting significantly thinner regions in nonpainted images compared to lesion in-painted images. Rows 1 and 2 show significant differences at $P = 0.01$, the right hemisphere showed a similar behavior. The different lobes are depicted in different colors: frontal (blue), temporal (yellow), parietal (green), occipital (red), and insula (brown). [Color figure can be viewed in the online issue, which is available at wileyonlinelibrary.com.]

reduces contrast between these two tissues that may affect the measured cortical thickness. Similarly, as the T1 values of lesions are higher than GM and WM, partial volume averaging with lesions that are proximal to the GM may also affect the tissue relaxation time and the measured cortical thickness

3. *Lesion segmentation*: Finally, almost all the automatic and semiautomatic segmentation algorithms classify the perilesional area as GM [Sajja et al., 2006; Shiee et al., 2014]. As pointed out by Magon et al. [2014], the proximity of these lesions to cortex introduces a segmentation bias which leads to incorrect estimation of cortical thickness measurements.

The effect of all the above factors can be mitigated to some extent by lesion in-painting. As a corollary, one would expect the effect of in-painting to decrease with lesion load. Indeed, this is consistent with our results.

We believe that this is the first study that showed that the effect of in-painting depends on the scanner field strength. Our results show that the effect of in-painting on the cortical thickness is more prominent at 1.5 T than at 3 T. The effect of field strength can be formally analyzed by recognizing that the value of T1 is field dependent [Bottomley et al., 1984]:

$$\mathrm{T1} = c + a * {B_0}^b \tag{2}$$

where a and b are tissue-dependent constants. Combining this expression and Eq. (1) yields CNR $\sim {B_0}^{1/2 - b/2}$. This simple model predicts that CNR increases with B_0. Since cortical thickness is determined by the distance between the lobar and cortical sheets' segmentation fidelity, it is expected that the effect of in-painting is more prominent at lower field.

In our study, we observed that the effect of in-painting is different between left and right hemispheres. There have been multiple studies that reported hemispheric asymmetry in the cortex [Lemaitre et al., 2012; Narayana

TABLE V. Multivariate regression on cortical thickness with and without in-painting on 918 RRMS patients divided by field strength

		In-painted		Nonpainted			
Lobe	Hemisphere	1.5 T ($n = 663$)	3 T ($n = 255$)	1.5 T ($n = 663$)	3 T ($n = 255$)	P-value[a]	P-value[b]
Frontal	Left	2.544 ± 0.248	2.556 ± 0.171	2.563 ± 0.237	2.553 ± 0.144	<0.001	0.104
	Right	2.558 ± 0.237	2.562 ± 0.171	2.561 ± 0.24	2.557 ± 0.146	0.551	0.504
Parietal	Left	2.310 ± 0.227	2.328 ± 0.174	2.320 ± 0.215	2.305 ± 0.164	0.148	0.052
	Right	2.328 ± 0.224	2.321 ± 0.172	2.321 ± 0.211	2.323 ± 0.157	0.321	0.447
Temporal	Left	2.672 ± 0.296	2.728 ± 0.23	2.711 ± 0.277	2.695 ± 0.172	<0.001	<0.001
	Right	2.726 ± 0.298	2.783 ± 0.242	2.754 ± 0.289	2.744 ± 0.185	0.002	<0.001
Occipital	Left	1.984 ± 0.227	1.894 ± 0.192	1.964 ± 0.212	1.961 ± 0.14	0.020	<0.001
	Right	2.028 ± 0.227	1.914 ± 0.164	2.003 ± 0.203	2.027 ± 0.148	0.005	<0.001
Cingulate	Left	2.609 ± 0.286	2.663 ± 0.22	2.655 ± 0.275	2.626 ± 0.171	<0.001	<0.001
	Right	2.617 ± 0.287	2.641 ± 0.219	2.642 ± 0.266	2.632 ± 0.179	0.010	0.070
Insula	Left	2.938 ± 0.312	2.999 ± 0.285	3.016 ± 0.321	2.960 ± 0.217	<0.001	0.054
	Right	2.957 ± 0.377	3.000 ± 0.26	3.007 ± 0.329	2.950 ± 0.237	0.005	0.078

[a]P-value is from testing mean difference between in-painted and nonpainted.
[b]P-value is from testing field strength between 1.5 T and 3 T.

TABLE VI. Multivariate regression on cortical thickness with and without in-painting on 918 RRMS patients divided by lesion load

		In-painted		Nonpainted			
Lobe	Hemisphere	Low lesion ($n = 459$)	High lesion ($n = 459$)	Low lesion ($n = 459$)	High lesion ($n = 459$)	P-value[a]	P-value[b]
Frontal	Left	2.572 ± 0.17	2.524 ± 0.274	2.593 ± 0.153	2.582 ± 0.263	0.001	<0.001
	Right	2.577 ± 0.172	2.541 ± 0.268	2.589 ± 0.15	2.569 ± 0.259	0.074	<0.001
Parietal	Left	2.347 ± 0.17	2.284 ± 0.249	2.360 ± 0.161	2.345 ± 0.234	0.103	<0.001
	Right	2.349 ± 0.168	2.304 ± 0.231	2.355 ± 0.155	2.328 ± 0.246	0.466	<0.001
Temporal	Left	2.705 ± 0.221	2.671 ± 0.326	2.753 ± 0.177	2.726 ± 0.31	<0.001	0.001
	Right	2.761 ± 0.229	2.724 ± 0.32	2.793 ± 0.193	2.778 ± 0.325	0.003	0.001
Occipital	Left	1.971 ± 0.198	1.948 ± 0.24	1.963 ± 0.173	1.935 ± 0.22	0.488	0.039
	Right	2.010 ± 0.188	1.983 ± 0.211	2.001 ± 0.172	1.982 ± 0.238	0.411	0.011
Cingulate	Left	2.633 ± 0.211	2.617 ± 0.315	2.671 ± 0.183	2.669 ± 0.303	0.001	0.172
	Right	2.638 ± 0.212	2.610 ± 0.293	2.661 ± 0.182	2.659 ± 0.317	0.049	0.017
Insula	Left	2.975 ± 0.365	2.935 ± 0.351	3.031 ± 0.301	3.044 ± 0.29	0.009	0.066
	Right	2.980 ± 0.36	2.958 ± 0.295	3.019 ± 0.317	3.010 ± 0.337	0.075	0.308

[a]P-value is from testing mean difference between in-painted and nonpainted.
[b]P-value is from testing T2 lesion volume of high and low.

et al., 2013; Plessan et al., 2014; Ramasamy et al., 2009; Thompson and Toga., 2003]. However, this is the first study that shows that the effect of in-painting is also asymmetric. As the lesion distribution appears to be symmetric between both hemispheres, it cannot be a reason for this aforementioned asymmetry. Thus, the reason for the observed asymmetric effect of in-painting on cortical thickness is unclear.

Our results suggest that lesion in-painting might be important only in the case of high lesion load (>6 ml in this study) but would have limited effect on patients with low lesion loads. Also, cortical thickness measurements based on images acquired at 1.5 T appear to be more affected by the presence of lesions than data acquired at 3 T. As can be seen from Tables V and VI, even for data acquired at 1.5 T in patients with high lesion load, the mean cortical thickness difference with and without in-painting is less than ~2%. As indicated above, the smaller effect of in-painting on cortical thickness at 1.5 T relative to 3 T could be due to higher CNR at 3 T compared to 1.5 T. We believe, based on our results on a large cohort, that the effect of in-painting on cortical thickness is mainly driven by the CNR which depends on the field strength. It is worth pointing out that the two earlier studies [Magon et al., 2014; Shiee et al., 2014] that reported the effect of in-painting on cortical thickness were performed at 1.5 T. Based on these results, it appears that in-painting has only small effect on the estimated regional and global cortical thickness.

Finally, it should be pointed out that our results are based on a group level analysis. However, the number of juxtacortical lesions, which are expected to have a more significant effect on the estimated cortical thickness compared to the periventricular lesions, varies from subject-to-subject. However, it is worth pointing out that based on the lesion probability maps shown in this manuscript (Fig. 6) and published literature [Holland et al., 2012] on large cohorts, the juxtacortical lesion load is significantly lower than the deep WM lesion load.

REFERENCES

Ballester C, Bertalmio M, Caselles V, Sapiro G, Verdera J (2001): Filling-in by joint interpolation of vector fields and gray levels. IEEE Trans Image Process 10:1200–1211.

Battaglini M, Jenkinson M, De Stefano N (2012): Evaluating and reducing the impact of white matter lesions on brain volume measurements. Hum Brain Mapp 33:2062–2071.

Bock NA, Hashim E, Janik R, Konyer NB, Weiss M, Stanisz GJ, Turner R, Geyer S (2013): Optimizing T1-weighted imaging of cortical myelin content at 3.0 T. Neuroimage 65:1–12.

Bottomley PA, Foster TH, Argersinger RE, Pfeifer LH (1984): A review of normal tissue hydrogen NMR relaxation times and relaxation mechanisms from 1–100 MHz: Dependence on tissue type, NMR frequency, temperature, species, excision, and age. Med Phys 11:425–448.

Calabrese M, Rinaldi F, Mattisi I, Grossi P, Favaretto A, Atzori M, Bernardi V, Barachino L, Romualdi C, Rinaldi L, Perini P, Gallo P (2010): Widespread cortical thinning characterizes patients with MS with mild cognitive impairment. Neurology 74:321–328.

Calabrese M, Grossi P, Favaretto A, Romualdi C, Atzori M, Rinaldi F, Perini P, Saladini M, Gallo P (2012): Cortical pathology in multiple sclerosis patients with epilepsy: A 3 year longitudinal study. J Neurol Neurosurg Psychiatry 83:49–54.

Ceccarelli A, Jackson JS, Tauhid S, Arora A, Gorky J, Dell'Oglio E, Bakshi A, Chitnis T, Khoury SJ, Weiner HL, Guttmann CR, Bakshi R, Neema M (2012): The impact of lesion in-painting

and registration methods on voxel-based morphometry in detecting regional cerebral gray matter atrophy in multiple sclerosis. Am J Neuroradiol 33:1579–1585.

Chard DT, Jackson JS, Miller DH, Wheeler-Kingshott CA (2010): Reducing the impact of white matter lesions on automated measures of brain gray and white matter volumes. J Magn Reson Imaging 32:223–228.

Charil A, Dagher A, Lerch JP, Zijdenbos AP, Worsley K, Evans AC (2007): Focal cortical atrophy in multiple sclerosis: Relation to lesion load and disability. Neuroimage 34:509–517.

Collins DL, Neelin P, Peters TM, Evans AC (1994): Automatic 3-D intersubject registration of MR volumetric data in standardized Talairach space. J Comput Assist Tomogr 18:192–205.

Dale AM, Fischl B, Sereno MI (1999): Cortical surface-based analysis. I. Segmentation and surface reconstruction. Neuroimage 9: 179–194.

Datta S, Sajja BR, He R, Wolinsky JS, Gupta RK, Narayana PA (2006): Segmentation and quantification of black holes in multiple sclerosis. Neuroimage 29:467–474.

Datta S, Sajja BR, He R, Gupta RK, Wolinsky JS, Narayana PA (2007): Segmentation of gadolinium-enhanced lesions on MRI in multiple sclerosis. J Magn Reson Imaging 25:932–937.

Datta S, Staewen TD, Cofield SS, Cutter GR, Lublin FD, Wolinsky JS, Narayana PA (2014): How important is the effect of lesion in-painting on regional atrophy in multiple sclerosis? In: Proceedings of the 22nd ISMRM, May 10-16, Milan, Italy.

Desikan RS, Segonne F, Fischl B, Quinn BT, Dickerson BC, Blacker D, Buckner RL, Dale AM, Maguire RP, Hyman BT, Albert MS, Killiany RJ (2006): An automated labeling system for subdividing the human cerebral cortex on MRI scans into gyral based regions of interest. Neuroimage 31:968–980.

Dickerson BC, Feczko E, Augustinack JC, Pacheco J, Morris JC, Fischl B, Buckner RL (2009): Differential effects of aging and Alzheimer's disease on medial temporal lobe cortical thickness and surface area. Neurobiol Aging 30:432–440.

Fischl B, Dale AM (2000): Measuring the thickness of the human cerebral cortex from magnetic resonance images. Proc Natl Acad Sci USA 97:11050–11055.

Fischl B, Sereno MI, Dale AM (1999): Cortical surface-based analysis. II: Inflation, flattening, and a surface-based coordinate system. Neuroimage 9:195–207.

Fischl B, Lui A, Dale AM (2001): Automated manifold surgery: constructing geometrically accurate and topologically correct models of the human cerebral cortex. IEEE Transactions on Medical Imaging 20:70–80.

Geurts JJ, Pouwels PJ, Uitdehaag BM, Polman CH, Barkhof F, Castelijns JA (2005): Intracortical lesions in multiple sclerosis: Improved detection with 3D double inversion-recovery MR imaging. Radiology 236:254–260.

Govindarajan KA, Freeman L, Cai C, Rahbar MH, Narayana PA (2014): Effect of intrinsic and extrinsic factors on global and regional cortical thickness. PLoS One 9:e96429.

Han X, Jovicich J, Salat D, van der Kouwe A, Quinn B, Czanner S, Busa E, Pacheco J, Albert M, Killiany R, Maguire P, Rosas D, Makris N, Dale A, Dickerson B, Fischl B (2006): Reliability of MRI-derived measurements of human cerebral cortical thickness: The effects of field strength, scanner upgrade and manufacturer. Neuroimage 32:180–194.

Hand DJ, Taylor CC (1987): Multivariate Analysis of Variance and Repeated Measures. London, UK: Chapman and Hall.

Holland CM, Charil A, Csapo I, Liptak Z, Ichise M, Khoury SJ, Bakshi R, Weiner HL, Guttmann CR (2012): The relationship between normal cerebral perfusion patterns and white matter lesion distribution in 1249 patients with multiple sclerosis. J Neuroimaging 22:129–136.

Krzanowski WJ (1988): Principles of Multivariate Analysis. A User's Perspective. London, UK: Oxford, Statistical Science Series.

Lemaitre H, Goldman AL, Sambataro F, Verchinski BA, Meyer-Lindenberg A, Weinberger DR, Mattay VS (2012): Normal age-related brain morphometric changes: Nonuniformity across cortical thickness, surface area and gray matter volume? Neurobiol Aging 33:617.e1–617.e9.

Lindsey JW, Scott TF, Lynch SG, Cofield SS, Nelson, F, Conwit R, et al. (2012): The CombiRx trial of combined therapy with interferon and glatiramer acetate in relapsing remitting MS: Design and baseline characteristics. Mult Scler Relat Disord 1: 81–86.

Lu H, Nagae-Poetscher LM, Golay X, Lin D, van Pomper M, Zijl PCM (2005): Routine clinical brain MRI sequences for use at 3.0 Tesla. J Magn Reson Imaging 22:13–22.

Magon S, Gaetano L, Chakravarthy MM, Lerch JP, Naegelin Y, Stippich C, Kappos L, Radue EW, Sprenger T (2014): White matter lesion filling improves the accuracy of cortical thickness measurements in multiple sclerosis patients: A longitudinal study. BMC Neurosci 15:106–115.

Narayana PA, Govindarajan KA, Goel P, Datta S, Lincoln JA, Cofield SS, Cutter GR, Lublin FD, Wolinsky JS, the CombiRX Investigators Group (2013): Regional cortical thickness in relapsing remitting multiple sclerosis: A multi-center study. Neuroimage Clin 2:120–131.

Nelson F, Datta S, Garcia N, Rozario NL, Perez F, Cutter G, Narayana PA, Wolinsky JS (2011): Intracortical lesions by 3T magnetic resonance imaging and correlation with cognitive impairment in multiple sclerosis. Mult Scler 17:1122–1129.

Olson CL (1974): Comparative robustness of six tests in multivariate analysis of variance. J Am Stat Assoc 69:894–908.

Olson CL (1976): On choosing a test statistic in multivariate analysis of variance. Psychol Bull 83:579–586.

Plessan KJ, Hugdahl K, Bansal R, Hao X, Peterson B (2014): Sex, age, and cognitive correlates of asymmetries in thickness of the cortical mantle across the life span. J Neurosci 34:6294–6302.

Ramasamy DP, Benedict RH, Cox JL, Fritz D, Abdelrahman N, Hussein S, Minagar A, Dwyer MG, Zivadinov R (2009): Extent of cerebellum, subcortical and cortical atrophy in patients with MS: A case-control study. J Neurol Sci 282:47–54.

Sailer M, Fischl B, Salat D, Tempelmann C, Schönfeld MA, Busa E, Bodammer N, Heinze HJ, Dale A (2003): Focal thinning of the cerebral cortex in multiple sclerosis. Brain 126:1734–1744.

Sajja BR, Datta S, He R, Mehta M, Gupta RK, Wolinsky JS, Narayana PA (2006): Unified approach for multiple sclerosis lesion segmentation on brain MRI. Ann Biomed Eng 34:142–151.

Sdika M, Pelletier D (2009): Nonrigid registration of multiple sclerosis brain images using lesion inpainting for morphometry or lesion mapping. Hum Brain Mapp 30:1060–1067.

Ségonne F, Dale AM, Busa E, Glessner M, Salat D, Hahn HK, Fischl B (2004): A hybrid approach to the skull stripping problem in MRI. Neuroimage 22:1060–1075.

Shiee N, Bazin PL, Cuzzocreo JL, Ye C, Kishore B, Carass A, Calabresi PA, Reich DS, Prince JL, Pham DL (2014): Reconstruction of the human cerebral cortex robust to white

matter lesions: Method and validation. Hum Brain Mapp 35: 3385–3401.

Smith SM (2002): Fast robust automated brain extraction. Hum Brain Mapp 17:143–155.

Thompson PM, Toga AW (2003): Mapping brain asymmetry. Nat Rev Neurosci 4:37–48.

Wonderlick JS, Ziegler DA, Hosseini-Varnamkhasti P, Locascio JJ, Bakkour A, van der Kouwe A, Triantafyllou C, Corkin S, Dickerson BC (2009): Reliability of MRI-derived cortical and subcortical morphometric measures: Effects of pulse sequence, voxel geometry and parallel imaging. Neuroimage 44:1324–1333.